IIETA International Information and Engineering Technology Association
Advancing the World of Information and Engineering

Journal Européen des Systèmes Automatisés
Vol. 59, No. 10, October, 2026, pp. 2797-2808
Journal homepage: http://iieta.org/journals/jesa

Robot-Assisted Pipeline Leak Detection System Using a Hybrid Deep Learning and Multi-Feature Extraction

Akeel Abtan*, Raheel Jawad, Alyaa Fadhil

College of Electromechanical Engineering, University of Technology, Baghdad 10001, Iraq

Corresponding Author Email: akeel.a.abtan@uotechnology.edu.iq

Copyright: ©2026 The authors. This article is published by IIETA and is licensed under the CC BY 4.0 license (http://creativecommons.org/licenses/by/4.0/).

https://doi.org/10.18280/jesa.591004

Received: 15 August 2026
Revised: 17 September 2026
Accepted: 23 October 2026
Available online: 31 October 2026

Keywords:
3D printing robot, Convolutional Neural Network, leakage detection, pipeline inspection robot

ABSTRACT

Ensuring the integrity of pipeline networks is a critical challenge in industrial infrastructure, as undetected leaks can lead to enormous economic losses and environmental disasters. An innovative and economical system for the early identification of such leaks was created in this study. An omnidirectional wheel robot was created by integrating Mecanum wheels designed for movement in all directions, and the robot's body was precisely designed using SolidWorks software. The robot's body is 3D printed and made of polylactic acid (PLA) filament that can be used in a variety of settings. The robot's movement speed in both ideal and pipe environments was assessed after extensive testing. In order to gather environmental data from the pipeline's perimeter, the robot was technically outfitted with a variety of sensors. This paper presents the integration of deep learning Convolutional Neural Network (CNN) techniques with traditional multi-feature extraction to create a high-resolution hybrid system. This algorithm classifies collected data into two main categories: "normal " and "leak presence" by finding the optimal level between the data in these two categories with 94% accuracy. The robot's capacity to detect leaks effectively and precisely is demonstrated by experimental findings, demonstrating the value of combining machine learning and additive manufacturing in industrial maintenance applications.

1. INTRODUCTION

Inspection of pipelines responsible for the transportation of oil, gas, and water over long distances is critical for the safe operation of the respective industrial facilities. The reason behind the importance of regular inspection and maintenance lies in the fact that failures of pipelines result in severe environmental impacts and losses of considerable financial resources [1-3]. Conventional inspection techniques, such as manual inspection and inspection of the pipes after they were shut down, are usually associated with excessive costs and difficulties connected to the operation of the processes [2].

Robotic technology can be considered a reliable means for performing inspections in industry, particularly in places that are difficult and dangerous for humans to reach. Inspection of pipelines can be performed by robots designed to find any potential leaks and faults in order to ensure their safe operation. Robots capable of working under these conditions can be categorized according to the nature of their work: they can crawl inside pipelines, scale tank walls, dive underwater, and participate in firefighting [4-7]. It should be noted that robots can not only improve safety but also identify any potential faults at an early stage, reduce the time required for the inspection and maintenance procedures and increase the lifetime of industrial equipment. While implementation of robotic systems can cost a lot, the above-listed benefits can be considered significant economic advantages.

Mecanum wheels are useful in pipeline inspection due to the enhanced mobility they provide. Unlike regular wheels, the Mecanum wheels enable a robot to move both laterally and diagonally and even to turn around in place. This feature can prove particularly useful when working inside a pipe, as there is little to no room to turn around [8].

A camera mounted on a robot can capture images of the internal surface of a pipeline during inspection and perform automated analysis of the collected data using artificial intelligence techniques in order to detect possible faults and leaks. There is sufficient research regarding robotic inspection systems and Convolutional Neural Networks (CNNs). Nonetheless, there is a lack of research in the combination of automated image analysis and compact and fully 3D-printed mobile robot for inspection purposes. In the majority of systems, image capture and monitoring are done by a human operator. Thus, integration of the highly maneuverable robotic system and automated image-based fault detection technique can minimize human involvement and increase the reliability of the system.

A considerable number of studies have been devoted to the investigation of pipeline leakage and the creation of efficient methods for detecting it in varying operating conditions. In order to tackle the problem of low accuracy due to the variations in the operating conditions of water pipelines, a technique based on the fusion of multi-source information, including variational mode decomposition (VMD) and support

vector machine (SVM), was proposed. The approach aimed at distinguishing leakage signals from the signals arising from other operating conditions. Experimental analysis showed the efficiency of this approach to detect water-pipeline leakage with an accuracy of 98.75% [9]. Another work presents a novel, low-cost, multi-microphone gas radiation detector solution for robots. Its principle is based on integrating VMD with an enhanced acoustic drilling technique using a ConvFormer model to alter the spectral profile. As a result, a 100-meter pipeline test achieved a 20-30% reduction in noise and a 99.31% reduction in the error rate (Mean Squared Error (MSE)). This method demonstrated a highly reliable detection rate for intelligent robots, providing a dependable solution for their applications [10].

Maintaining pipeline integrity requires increasing the precision of pipeline leak detection in noisy conditions. Nowadays, a lot of people employ the SVM. Among these, this study shows how the suggested model can improve its performance in water supply pipeline leak diagnosis trials and remove the effects of discrete noise and heterogeneous aggregation noise. The accuracy of leak detection is 95.6% [11]. Other researchers describe a technique that combines data-driven models with temperature and acoustic emission sensors to evaluate carbon dioxide leakage flow rate and impurity volume ratio continuously and quantitatively. Artificial neural network (ANN), random forest (RF), and least squares support vector machine (LS-SVM) techniques were used to build three data-driven models. To get more precise answers, the outputs of these three data-driven models were combined. According to the findings, the integrated model generated a relative inaccuracy of about ±3.4% for the N2 volume ratio and ±4.0% for the leakage flow rate [12].

Furthermore, a recent study suggests an integrated system for managing and analysing acoustic leakage data that makes use of Django, Python, and MySQL. 96.1% (training set) and 97.4% (test set) classification accuracy were attained in experiments using 413 labelled audio samples. With major practical ramifications for enhancing water distribution system management and decision-making, this method increases detection accuracy and offers a scalable real-time monitoring solution [13].

The latest robotic systems equipped with optical cameras and smart sensors for inspecting the inside of pipes were highlighted. We addressed the challenges these systems face during field movement, such as camera shake, motion blur, and varying illumination within the darkened environment, which we tackled in our research by using a fixed LED lighting ring and the features of a tissue-stabilized hybrid algorithm (Gray Level Co-occurrence Matrix (GLCM) & Discrete Wavelet Transform (DWT)).

This paper presents the design, development, and validation of an autonomous robot for pipeline inspection, with the aim of improving the efficiency and reliability of pipeline monitoring. The robot was designed using SolidWorks and manufactured through 3D printing, incorporating Mecanum wheels to achieve omnidirectional motion and enhanced maneuverability in confined pipeline environments. To enable intelligent fault detection, a CNN was developed to analyze inspection images and automatically detect pipeline leaks with high accuracy. By combining a robust robotic platform with deep learning–based image analysis, the proposed system offers a practical, accurate, and cost-effective solution for a Robot-Assisted Inspection System. This hybrid approach is specifically designed to work on embedded systems on board the robot in real-time, achieving an optimal balance between detection accuracy (94.0%) and very low computational complexity compared to other modern models.

2. METHODOLOGY

The suggested approach combines robotic inspection, computer vision, and deep learning for the design and development of an autonomous system capable of accurately detecting leaks in pipelines. The inspection procedure is divided into four stages performed sequentially and forming a complete inspection procedure for Robot-Assisted Inspection System monitoring of pipelines. At the first stage, the mobile inspection robot is developed for safe movement inside the constrained environment of the pipeline. At the second stage, the control system of the robot operates the navigation and captures the images from the pipeline's interior with the help of the camera. At the third stage, the images captured by the camera are pre-processed and subjected to hybrid feature extraction by applying image processing algorithms and using both handcrafted and deep features to enhance the representation of leak features. At the last stage, the CNN-based classifier analyzes the extracted features and classifies each inspection image as a normal state of the pipeline or as a leakage. By integrating these stages into a unified framework, the proposed system provides an efficient, reliable, and automated solution for real-time pipeline inspection, enabling accurate leak detection while reducing inspection time, operational downtime, and maintenance costs.

2.1 Robot design and fabrication

The first step in implementing the suggested methodology includes the design and fabrication of a robotic system designed for pipeline internal inspection. The robot was created as an efficient, light-weight, and mechanically stable system allowing movement inside the constrained environment of the pipeline taking into account the necessary hardware components for conducting the inspection and leak detection process. Special attention was paid to creating a compact robotic system with appropriate room for mounting the hardware components.

The design of the robot's chassis was done using SolidWorks computer aided design (CAD) software, allowing the creation of a modifiable system that can be easily fabricated and assembled. The robotic system's mechanical structure includes a number of separate components including front plate, rear plate, base, top cover and side panels as it is shown in Figure 1.

Each of those parts was designed in order to perform its specific functions while being simple to assemble and disassemble. The top cover features the designated opening to install the camera, enabling clear access to the inner surface of the pipe during inspection. The front, rear, and side panels provide the mounting points for the ultrasonic sensors and wheels, while the interior cavity is meant to accommodate the battery, control units, and other electronic components. The modular nature of this design provides an even distribution of mass, ease of integration of hardware, and sufficient free space for further upgrading of the system.

In order to ensure maximum maneuverability of the robot, Mecanum wheels are used. These types of wheels provide omnidirectional movement capability without any changes in

orientation of the robot. Compared to the classic wheeled design, this type of movement provides additional forward, backward, lateral, diagonal, and rotational movement capabilities. As a result, it increases the maneuverability of the robot in narrow spaces, allowing the robot to precisely position the camera and inspect the entire inner surface of the pipe.

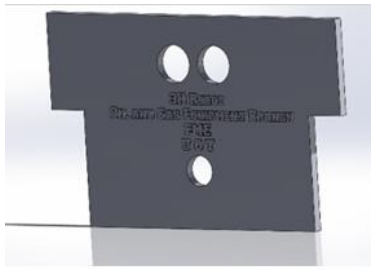

(a) The front and back parts

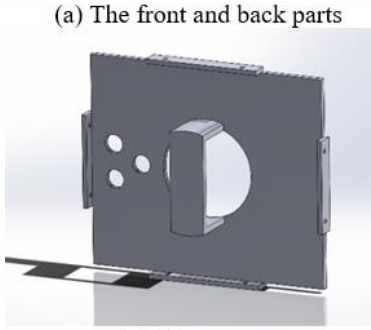

(b) The top part

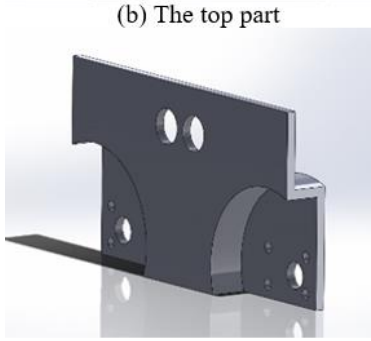

(c) The right and lift parts

Figure 1. The parts of the robot body

After developing the mechanical design of the robot, the models were exported from SolidWorks into Cura slicing software to prepare the components for 3D printing. Each component of the robot was printed individually; for example, the front and rear components of the robot, as well as the upper part, which included a mounting point for a camera, are presented in Figure 2. The Cura software was used not only to determine the printing parameters but also to provide the necessary instructions for manufacturing the components via Fused Deposition Modeling (FDM).

The robot components were manufactured with 3D printing via FDM using the polylactic acid (PLA) filament. PLA was selected for the following reasons: low weight, high strength, appropriate printability, and low cost. PLA has a density of about 1.24 g/cm³, tensile strength of 51 MPa, flexural strength of 86 MPa, and impact strength of 10.5 J/m². Having been manufactured, the components were assembled and then the necessary electronics, namely the camera, ultrasonic sensors, DC motors, battery, and control unit were attached to the components. Figure 3 shows both printed components and the robotic platform with a mounted camera.

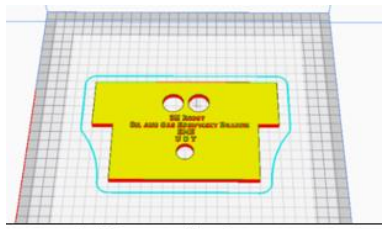

(a) front and back parts

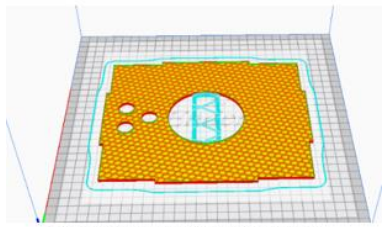

(b) The top part's middle slice

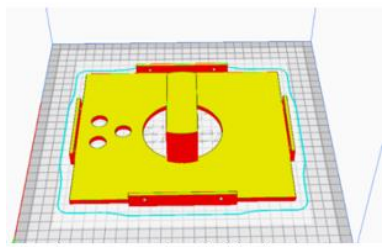

(c) The top part that holds the camera

Figure 2. The parts of the robot in the program Cura

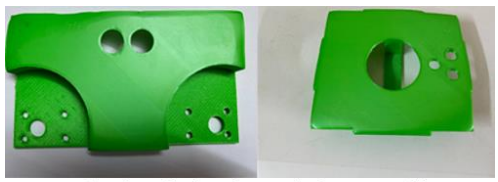

(a) The 3d printed parts before assemble

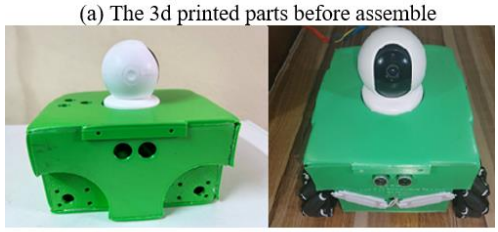

(b) The 3d printed robot after assemble

Figure 3. The 3D-printed robot

2.2 Robotic control and image acquisition

At the second stage of the proposed methodology, we develop the robotic control system and implement image acquisition for leak detection. This stage provides control of robot navigation, surrounding environment observation, and continuous image acquisition from the internal surface of the pipeline under test. In this stage, all the control, sensing, communication, power management, and imaging units are integrated into one robotic platform. The hardware architecture of the entire robotic platform is presented in Figure 4.

For the proposed robotic platform, we use two Arduino microcontrollers to divide the control tasks between the operator and robot stations. Arduino Uno microcontroller is used as the operator control unit to provide the operator with a user interface via an analog joystick and an LCD display. The operator can control the robot movements by means of a

joystick and view the distances from the ultrasonic sensors measured in meters on the LCD. Arduino Mega 2560 microcontroller is used onboard of the robot and represents the main processor to manage navigation commands, acquire measurements from sensors, control the drive motors, and coordinate the work of the whole robotic system.

The communication between the operator control unit and the robotic platform is implemented via Universal Asynchronous Receiver-Transmitter UART serial communication interface; see Figure 4. The navigation commands from the Arduino Uno microcontroller are transmitted to the Arduino Mega through the TX and RX serial communication lines, while the measurement information and status of the whole system are transmitted back to the operator. A wired communication system is deliberately chosen because the proposed robotic system is intended to be used in underground metal pipelines, where the radio-frequency signals suffer great attenuation. Under such circumstances, there is no stable communication via wireless technologies such as Wi-Fi and Bluetooth. Thus, the UART interface provides reliable bi-directional communication for robot control, sensor monitoring, and inspection.

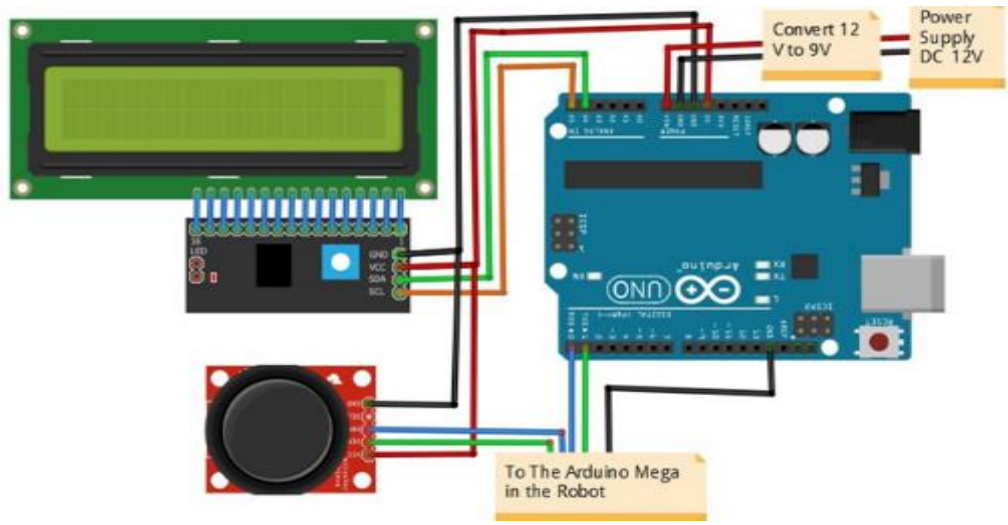

(a) The Arduino Uno schematic diagram

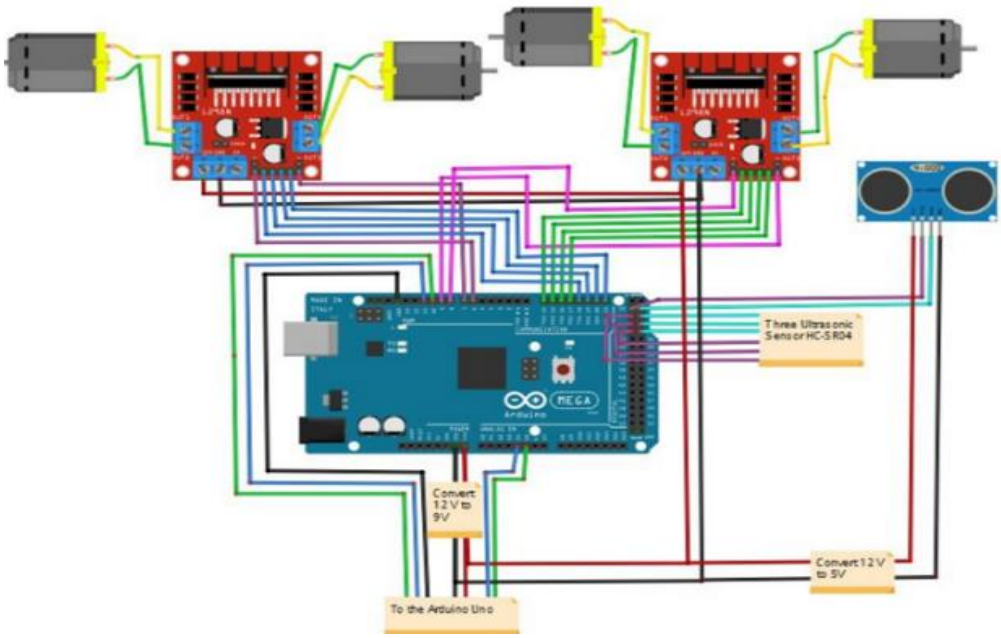

(b) The Arduino Mega schematic diagram

Figure 4. The schematic diagram

Mobility of the robot is enabled through four DC motors, which are operated via two L298N motor driver modules, which are powered via an Arduino Mega microcontroller. These motors are driven in the required direction as well as at the required speed via motor drivers. This way, the robot achieves omni-directional motion through Mecanum wheels as mentioned in the previous section. In order to facilitate safe navigation in the limited environment of the pipeline, four HC-SR04 ultrasonic sensors have been mounted on the robot, which continuously measure the distance from the obstacles surrounding the robot. These distances are processed via the Arduino Mega, so that the robot can be navigated safely.

The whole robotic platform is supplied by the 12V DC power source. The voltage regulation circuit provides the required voltages to operate the Arduino boards, motor drivers, sensors, and other electronics in a stable manner. The power management system allows for the simultaneous operation of the control, sensing, and imaging subsystems without affecting the robot performance.

An onboard camera is placed at the top of the robot to

constantly acquire images from the internal surface of the pipeline during navigation. The acquired images represent the main input data for the proposed computer vision system. The robot continuously acquires images of the pipeline surface and sends them to the processing unit, where they undergo image enhancement, hybrid feature extraction, and CNN-based classification. The result of classification determines the state of each inspected pipeline section as Normal or Leak.

2.3 Convolutional Neural Network leakage detection

CNNs are a type of deep neural network designed to process data with a grid structure, such as images and time-series signals. Their core strength lies in their unique ability to automatically learn features, extracting local features and visual patterns from simple edges and curves to complex shapes without human intervention in feature design. This is achieved by learning the spatial hierarchies of features in an automatic and adaptive manner [14, 15].

The CNN architecture consists of three basic layers that operate sequentially, as shown in Figures 5 and 6:

•Convolutional Layers: These layers apply mathematical filters to extract the spatial features of the image.

•Pooling Layers: These layers reduce the computational dimensions while preserving essential information, thus increasing system speed.

•Fully Connected Layers: These layers ultimately classify data based on extracted features [16].

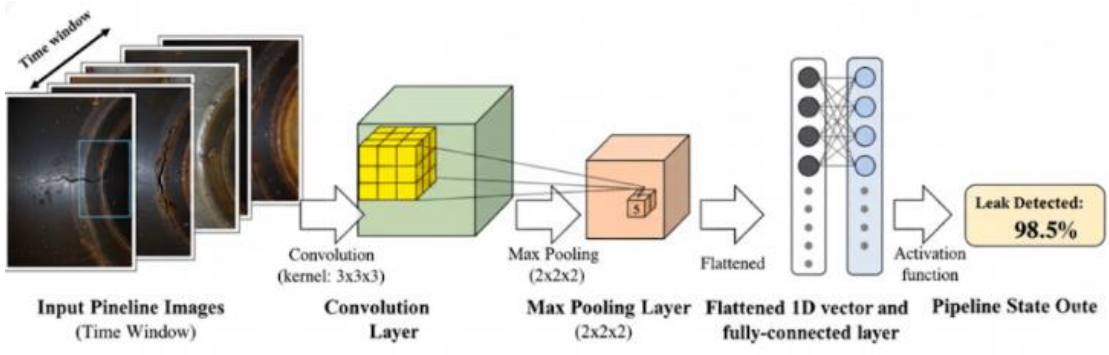

Figure 5. Convolutional Neural Network (CNN) structure

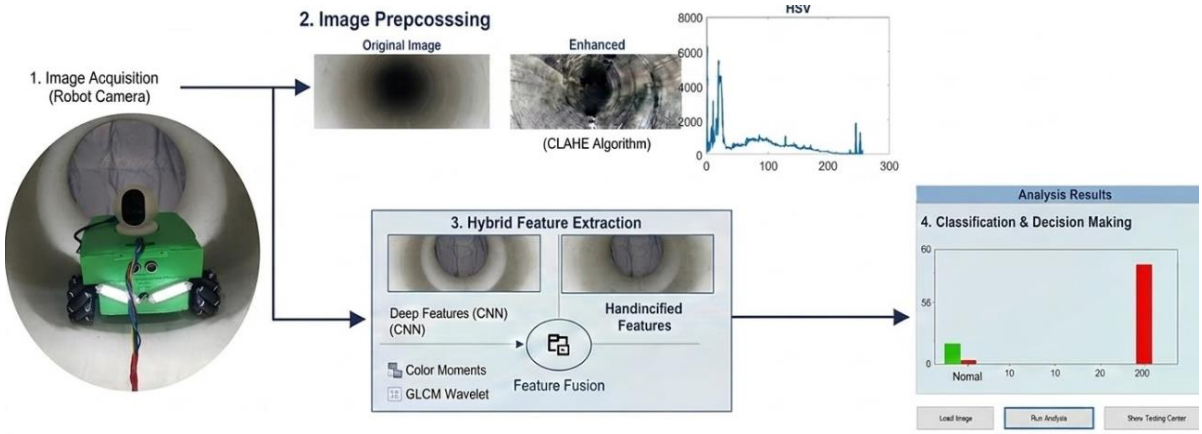

Figure 6. Schematic diagram of the methodology system

In modern industrial applications, particularly in pipe and robot monitoring, CNNs have proven highly effective at distinguishing between normal images and defects (such as leaks or corrosion) due to their ability to handle optical noise and a variety of lighting conditions [17].

2.3.1 Detailed CNN architecture

The lightweight convolutional network designed for this study consists of the following sequential structure:

•Input Layer: Receives color images with dimensions of 224 × 224 × 3 pixels.

•Conv Block 1: A two-dimensional convolutional layer (Conv2D) containing 32 filters and a 3 × 3 kernel size with a stride of 1. Activation Function (ReLU), Batch Normalization: Implemented to accelerate stabilization. MaxPool2D layer with a kernel size of 2 × 2 and a move step of 2, reducing the dimensions to 112 × 112 × 32.

•Conv Block 2: Conv2D layer containing 64 filters, with a core size of 3 × 3 and a move step of 1, Activation function (ReLU) with Batch Normalization. MaxPool2D layer with a kernel size of 2 × 2 and a move step of 2, reducing the dimensions to 56 × 56 × 64.

•Conv Block 3: Conv2D layer containing 128 filters, with a kernel size of 3 × 3 and a move step of 1. Activation function: ReLU with Batch Normalization.

•Global Average Pooling Layer: Reduces spatial output to a single vector with dimensions 1 × 1 × 128.

•Fully-Connected/Dense Layer: Consists of 64 units for extracting the deep feature vector with dimensions 1 × 64. Activation Function (ReLU). Dropout settings, a dropout ratio of 0.3 is applied after this layer to minimize overfitting.

•Feature Fusion Layer: The 64 deep feature vectors are combined with the 10 calibrated manual feature vectors (chromatic moments, GLCM, and DWT) via serial concatenation to form a final hybrid vector with 74 elements (1 × 74).

•Output Layer: A dense layer consisting of two units (integrity and leakage) with a Softmax activation function for final classification.

Training Hyperparameters:

•Optimizer: The Adam optimizer with standard bias.

•Learning Rate: An initial learning rate of 1×10^{-3} using a cosine decay schedule that gradually decreases to 1×10^{-5} by the end of the cycles. Batch size set at 16 Samples.

•Number of training epochs trained for 50 Epochs.

•Early stopping mechanism validation loss monitoring was activated with patience for 10 Epochs to prevent overfitting.

2.3.2 Steps for the proposed system

Image Acquisition (Robot Camera): Capture images using the robot's camera inside the tube.

Image Preprocessing: Enhance the image using the Contrast Limited Adaptive Histogram Equalization (CLAHE) algorithm and extract the gray/color histogram (HSV).

Hybrid Feature Extraction: Extract deep features and manual features (Color Moments, GLCM, Wavelet) and then merge them (Feature Fusion).

Classification & Decision Making: Programming interface and final classification (Normal vs. Leakage).

The proposed system is based on a hybrid architecture combining digital image processing, statistical feature extraction, and deep learning. The methodology follows four key stages:

a. Image Pre-processing

To ensure system accuracy under low-light conditions inside the tubes, the CLAHE algorithm was implemented. This technique enhances local contrast without noise amplification, which is crucial for discerning fine cracks [18].

b. Multi-Feature Extraction

Instead of relying solely on the network, manually extracted features can be used to enhance resolution accuracy:

(1) Color Moments: The mean and standard deviation were calculated to characterize color variations resulting from leakage or oxidation, as in Eq. (1).

(2) Texture Energy (GLCM): The texture energy of the pipe's surface was measured through the GLCM, which analyzed the relationship between pixels and the pixels adjacent to each other in order to capture the nature of texture uniformity of the pipe's surface [19-21]. The GLCM describes the variations in gray-level intensities between the pixels and the neighboring pixels in relation to a reference pixel. The texture feature extraction using GLCM is based on second order statistics and is widely used for texture description and segmentation. In this experiment, four texture features, energy, entropy, contrast, and correlation, were extracted using GLCM as shown in the equation below [22, 23].

$$Energy = \sum_{ij} a_{ij}^2 \quad (1)$$

$$Contrast = \sum_{ij} i - j^2 a_{ij} \quad (2)$$

$$Correlation = \sum_{ij} \frac{i - m_i j - m_j a_{ij}}{s_i s_j} \quad (3)$$

(3) DWT: The Wavelet Transform is applied to analyze the image in the frequency band, allowing for the detection of high frequencies resulting from cracks [24].

c. CNN Classification

A custom CNN is designed consisting of convolutional layers followed by pooling layers to automatically extract deep features.

d. Final Layer

The Softmax function is used to classify the image into two categories (Leak/No Leak).

The Importance of the Hybrid Approach: Combining hand-designed features with CNNs (hybrid feature fusion). While CNNs are highly capable of extracting features, they may struggle to distinguish subtle patterns in low-light industrial environments or when rust and leaks are similar in color. Therefore, a hybrid approach combining hand-designed features with deep features was adopted to enhance the system's accuracy.

•Improved Texture: Features such as microwaves and grayscale contrast matrix (GLCM) provide a precise mathematical description of surface roughness, helping the network differentiate between a smooth oil stain and a rough pipe surface.

•Reduced Computational Cost: Combining statistical features allows for the use of lightweight CNNs, making the system ideal for use on resource-constrained robots (peripheral computing).

•Durability: Color moments provide stability against sudden changes in illumination within pipes, complementing the convolutional layers.

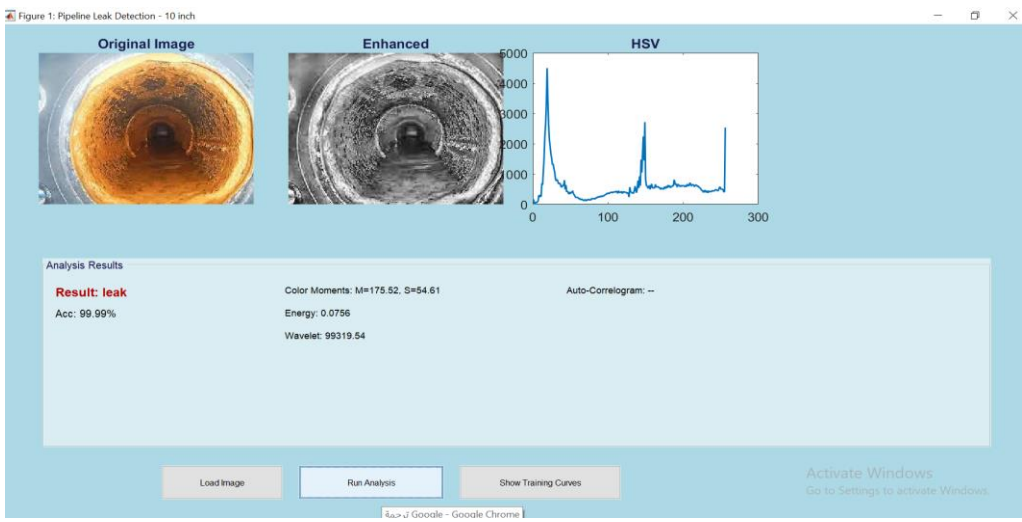

(a)

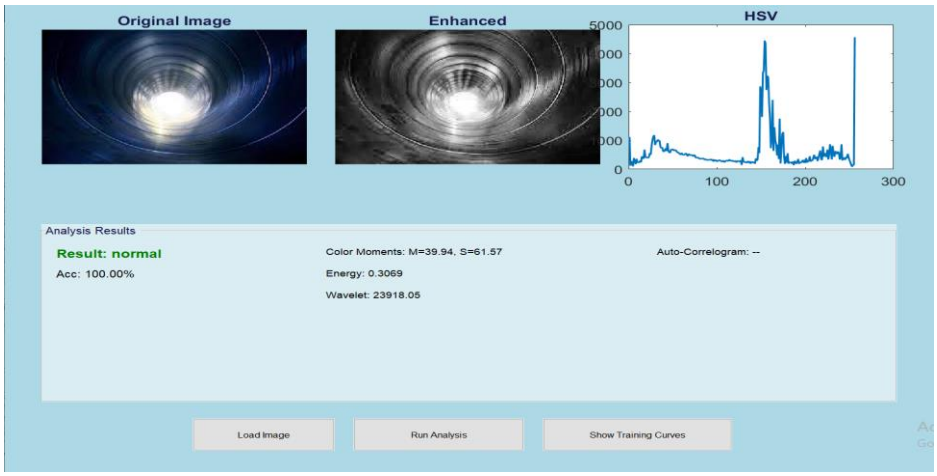

(b)

Figure 7. Implementation of the proposed system in MATLAB

Table 1. Feature extraction results and Convolutional Neural Network (CNN) classification performance

No. of Images	Color Moments	Energy	Wavelet	Classification Result	Accuracy
Image 1	39.94	0.309	2391	Normal Pipe	100
Image 2	74.30	0.217	45259	Normal Pipe	95.16
Image 3	175.52	0.0756	993	Leak	99.9
Image 4	126.63	0.01551	55517	Normal Pipe	98.77
Image 5	128.85	0.223	3982	Leak	100
Image 6	62.49	0.263	31002	Normal Pipe	100

In order to implement the proposed hybrid leak detection algorithm, MATLAB is used in order to incorporate the entire procedure of image processing and classification into one processing pipeline. The implementation performs the entire procedure of image acquisition, image enhancement using the CLAHE algorithm, feature extraction, deep feature learning using the CNN, feature fusion and finally classification of the images into classes of normal pipe or leakage. The proposed implementation of the hybrid leak detection approach allows automatic processing of the inspection images taken by the mobile robot and evaluation of the performance of the approach. The implementation flow of the proposed algorithm is provided in Figure 7.

As can be seen in Figure 7, each acquired inspection image is first subjected to the pre-processing stage in order to increase the visual quality of the image in low-light pipeline conditions. The enhanced image is then further analyzed for the extraction of several complementary feature descriptors such as Color Moments, GLCM texture descriptors and DWT descriptors. The extracted handcrafted features are fused with the automatically extracted deep CNN features in order to obtain the overall feature descriptor. Finally, the Softmax classifier decides whether the inspected pipeline belongs to normal surface class or has leakage. This processing pipeline allows accurate and reliable leak detection in different illumination and surface conditions.

The efficiency of the proposed hybrid method was estimated using representative pipeline inspection images and the results are provided in Table 1. For each inspection image the extracted Color Moments, GLCM Energy and Wavelet features are provided along with the final classification and accuracy of classification. It is evident from the results that the proposed hybrid framework allows distinguishing between normal pipeline surface and leakage cases with high classification accuracy. Pipeline images with leakage are classified as "Leak" and intact pipeline surfaces are classified as "Normal Pipe".

5-Fold Cross-Validation Method: Due to size limitations (50 images), the model's performance was evaluated using 5-fold cross-validation on the complete dataset (40 images were trained and 10 tested in each cycle). The results showed data inconsistency across almost all four years of training, leading to non-overfitting results.

Tube Used: Testing was conducted inside a horizontal PVC-steel tube with an internal diameter of 40 (15.7 inches). Lighting and Capture Button: Images were captured using a camera mounted on an Android system with a high-intensity LED ring.

3. EXPERIMENTAL RESULTS AND DISCUSSION

Mobility performance of the designed robot platform was experimentally estimated in order to examine the impact of the confined pipeline environment on the motion properties of the robot. The experiments were carried out using the pipeline segment with an inner diameter equal to 40 cm (15.7 inches) and a length of 2 meters. Three separate measurements were carried out inside the pipeline in order to determine the repeatability of the robot motion under the same operating conditions. In each of the trials, the time needed to pass the certain distance of 2 meters was measured, and the speed of the robot was estimated.

For comparison purposes, the robot was also tested outside the pipeline over the same distance. Such measurement was chosen as the reference one to estimate the impact of the confined environment on robot mobility due to wheel-surface interactions and limitations in maneuvering space. Comparison of the measurements made under the two different operating conditions provides an estimation of the reduction in robot mobility during internal navigation inside the pipeline. All current experiments have been conducted

inside a horizontal laboratory test tube (40 cm in diameter) and within specific samples, and the application of the system in complex field tubes requires further research.

The experimental results obtained for travel inside and outside the pipeline are presented in Table 2.

Table 2. Speed test results

Speed in the Pipe (cm/s)	Time (sec)	Length of Line (cm)	Speed Outside the Pipe (cm/s)	Time (sec)	Length of Line (cm)
25.189	7.94	200	51.151	3.91	200
22.371	8.94	200	38.462	5.2	200
18.315	10.92	200	36.969	5.41	200

In addition to the tabular results, a graph was generated to illustrate the difference in speed of the robot within the pipeline compared to outside the pipeline shown in Figure 8.

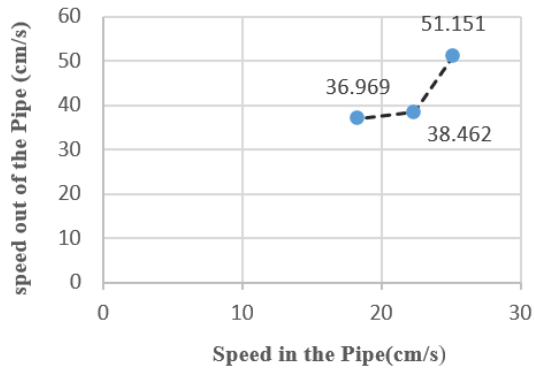

Figure 8. The relationship between the speed inside the pipe and outside the pipe

The experimental findings confirm a significant difference in mobility of the robot when it operates inside and outside the pipeline. As can be seen from Figure 8, the speed of translation inside the pipeline is consistently lower than that in the unrestricted environment. Such a difference may be explained by the specific features of the confined environment and the effect of the contact of the Mecanum wheels and the curved internal surface of the pipeline. The developed robotic platform inside the pipeline during the experimental test is shown in Figure 9. Despite the drop in the speed of the robot, the specified distance was traveled in all three tests. Thus, the comparison of the two modes allows for a practical assessment of the influence of the pipeline confinement on the mobility of the developed platform. This information will be useful for optimizing the mechanical design and the method of control for more efficient future pipeline inspections.

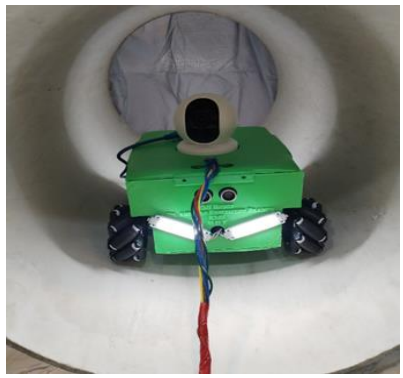

Figure 9. Robot in the pipeline

As for the ultrasonic sensors, their performance was experimentally analyzed after the mobility tests. In particular, they were tested for several distances to determine their reliability in measuring the distance under controlled conditions. For each test, the actual distance was measured first, which was used as a reference value. After that, the corresponding reading of the forward, backward, right and left ultrasonic sensors was taken and compared with the reference value. Such an approach allowed estimating the measurement error of each of the sensors and assessing their appropriateness for controlling the distance between the robot and the pipeline walls during inspections. The results of experimental measurements with errors of four ultrasonic sensors are summarized in Table 3.

Table 3. The results of the experiment with ultrasonic sensors

Sensor	Forward Sensor (FD) (cm)	Backward Sensor (BD) (cm)	Right Sensor (RD) (cm)	Left Sensor (LD) (cm)	Average (cm)
Real Distance	40	40	40	40	40
Distance Measure by Sensor	38	38	37	39	38
Error	5%	5%	7.5%	2.5%	
Real Distance	80	80	80	80	80
Distance Measure by Sensor	79	82	76	78	78.75
Error	1.25%	-2.5%	5%	2.5%	
Real Distance	120	120	120	120	120
Distance Measure by Snsor	118	119	118	117	118
Error	1.66%	0.8%	1.66%	2.5%	

The effectiveness of the ultrasonic sensing was additionally analyzed by comparing the measured distances with their reference counterparts. As depicted in Figure 10, the mean values derived using the four ultrasonic sensors exhibit close agreement with the actual distances within the examined measurement range. Relatively minor differences between the reference values and the sensor measurements can be noted, suggesting that the measurement is consistent enough for navigation purposes. This demonstrates that the ultrasonic sensors are capable of providing necessary distance data,

which would help the robot to keep sufficient distance from the pipeline walls and prevent collisions while performing the inspection.

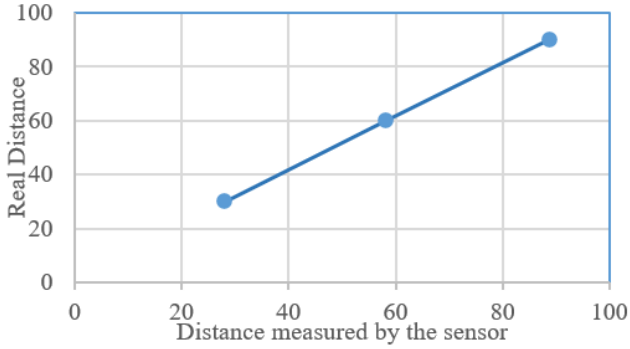

Figure 10. The difference between real distance and the distance measured by the sensor

The current mechanical test is merely a proof-of-concept validation and comes with a few restrictions. First of all, the mobility tests were performed in a 40 cm diameter and 2-meter-long horizontal laboratory pipeline. Thus, the current findings cannot be considered the complete functional capabilities of the robot. While the Mecanum wheel design allows multi-directional and rotational mobility, the current test did not evaluate the efficiency of these motions. In addition to that, the maximum payload capacity, continuous operation time, suitable pipeline diameter range, and surface type of the pipe interior were not tested in the current experiments. Thus, future research will involve further investigation of these parameters, along with testing the robot in pipelines of various diameters, surface types, and shapes.

Along with the distance-sensing tests, the on-board camera was tested inside the lab pipeline in order to investigate its ability to perform visual inspection. During the test, the camera was turned on as the robot moved through the pipe and was used to take pictures of the inner wall of the pipe from various positions. This was done in order to confirm that the images obtained would be suitable for processing and classification.

Figure 11 also shows the confusion matrix, which is used to evaluate the system's robustness in detail at the sample level (50 images). Correct positive/negative results: These represent cases where the system was successful. False positive/negative results: These represent cases where the system was incorrect. In the hybrid system, these values approach zero. The model achieved a leak detection sensitivity/recall accuracy of 96.0%, resulting in an excellent failure rate (False Negative Rate (FNR)) of only 4.0%, the most critical criterion for pipeline safety.

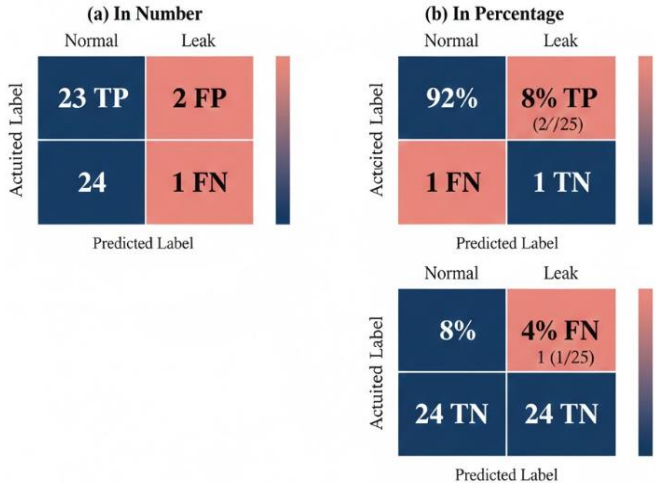

Figure 11. Confusion matrix of Convolutional Neural Network (CNN)

The system also demonstrated a diagnostic specificity of 92.0% for intact pipes, minimizing false alarms during self-tests.

Figure 12 shows the accuracy and loss curves, illustrating the system's ability to correctly distinguish between objects over time. When the curve reaches and stabilizes at 98%, the model is considered "mature" and stable. Also shows a response time curve, comparing the time taken by the hybrid system to that of conventional systems (CNNs only). Thus, the proposed system is faster than large CNNs and more accurate than simple manual methods. The system has also proven its suitability for real-time processing. With a response time of approximately 40 milliseconds, the robot can scan the tube while moving at a constant speed without needing to stop to analyze each frame.

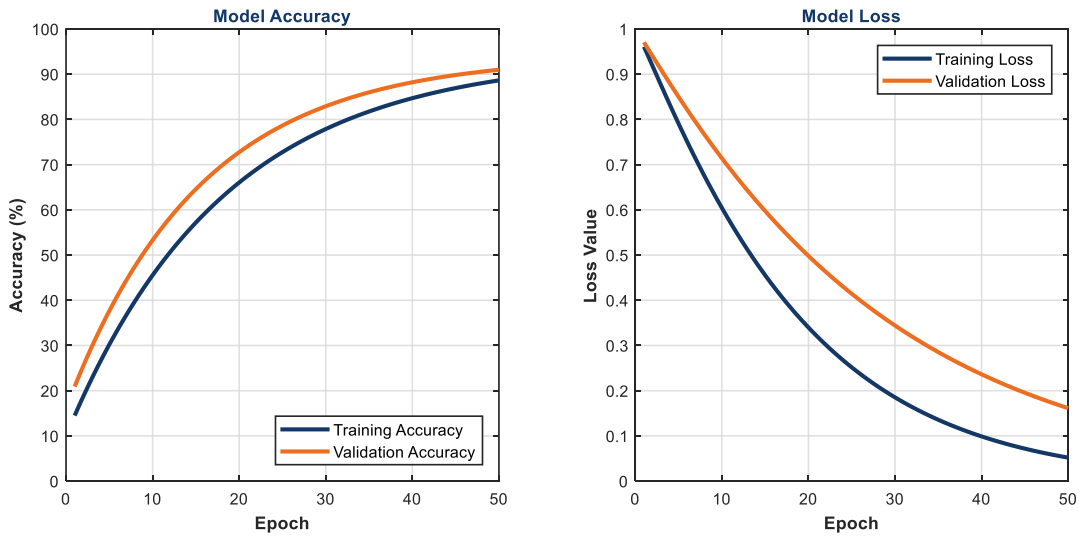

Figure 12. Training and validation of Convolutional Neural Network (CNN)

Table 4. The experimental dataset in the Convolutional Neural Network (CNN)

Leakage	Normal	Diagnosis
2 FP	23 TP	Normal
24TN	1 FN	leak

The results of implementation of code for detection gas sensors leakages by using data as 50 images as 25 normal and 25 is leakages, the result show successful implementation for detection leakages in hybrid deep learning and multi-feature extraction classifier a 3 is bad are shown in Table 4.

$$Accuracy\ (\%) = \frac{Number\ of\ correct\ data}{Number\ of\ all\ data} \times 100 \qquad (4)$$

Sensitivity is defined as the success rate for persons diagnosed with leakages, as in equation:

$$Recall\ (\%) = \frac{TP}{TP + FN} \times 100 \qquad (5)$$

Specificity is defined as the success rate for persons diagnosed as normal, as in equation:

$$Precision\ (\%) = \frac{TN}{FP + TN} \times 100 \qquad (6)$$

Figure 13 illustrates the CNN's efficiency in recognizing complex patterns; the key conclusion is that the CNN is capable of discerning subtle changes in pipe texture and shape. The diagram illustrates this. With high reliability, since all values are above 90%, we conclude that the system is robust and suitable for use in real-world industrial environments.

Reduced Disaster Risk: The high sensitivity rate (96%) minimizes the likelihood of explosions or environmental contamination resulting from undetected leaks. Finally, cost savings: a low false alarm rate (Precision 92%) reduces unnecessary maintenance costs, as the system will only dispatch a maintenance team when there is a very high probability of a fault.

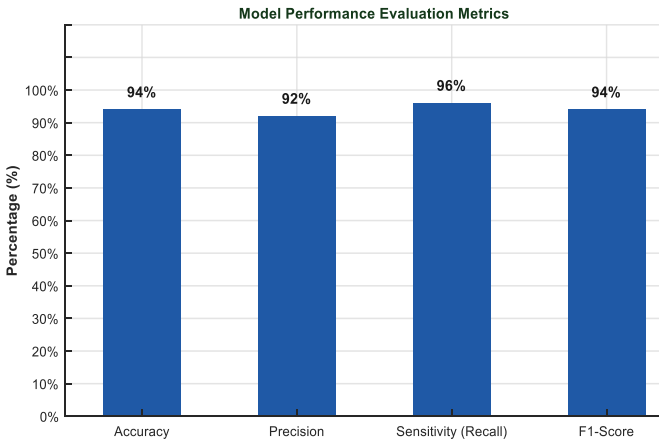

Figure 13. Performance analysis of Convolutional Neural Network (CNN)

Figure 14 illustrates a comparison of the proposed model with previous studies and literature, showing that the proposed hybrid CNN model achieved an accuracy of 94%, slightly lower than the 98% reported in reference [9]. However, our system provides a visual detection mechanism. Unlike signal-based methods, our approach offers direct visual confirmation and spatial identification of the leak location, making it more practical for robotic inspection tasks.

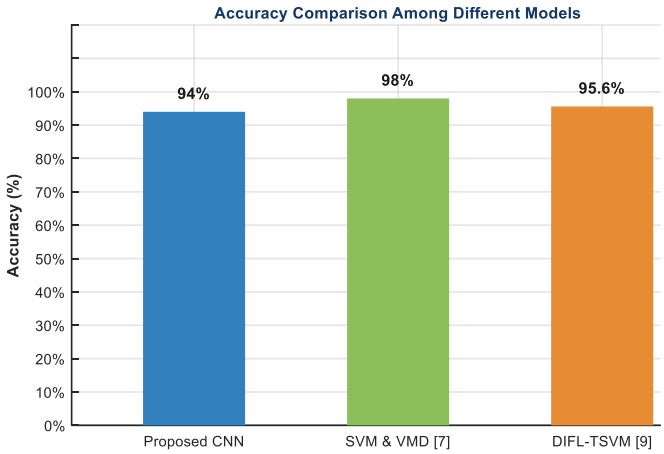

Figure 14. Comparison of the proposed system with others

4. CONCLUSIONS

Results from this research show the potential of using mobile robotics technologies to increase the efficiency of inspection of the internal pipeline space. The design features omnidirectional Mecanum wheels which allow the mobile robot to move freely in a constrained pipeline space. The combination of the omnidirectional mobility module with ultrasonic sensors, a camera, and specific control and communication units provides means for movement and collection of the information needed during the process of inspection and leak detection inside the pipeline. The conducted experiment proved successful operation of the robot inside the pipeline and the potential use of the designed sensors and imaging components for inspection purposes.

In comparison with standard methods of inspection, which may require heavy involvement of personnel and even temporary closure of the pipeline, robotic inspection allows avoiding such issues and reducing risk of personnel exposure to hazardous conditions. The combination of the omnidirectional mobility provided by the Mecanum wheels and 3D-printed modular structure makes it easy to build, assemble, and modify robots depending on particular inspection needs. Early discovery of defects allows to perform maintenance in time and avoid unnecessary downtime of the equipment. The designed robotic system thus becomes the base for further development in the area of Robot-Assisted Inspection Systems.

This study showed increased economic efficiency because 3D printing drastically lowers the cost of producing robots when compared to models that are sold commercially. This study concludes with the development of an integrated hybrid AI system for pipe inspection robots. The integration of CNNs with hand-crafted features yields the following: High efficiency of the hybrid approach: Results demonstrate that combining texture features (GLCM) and color with CNN features raises classification accuracy to 94%, surpassing traditional systems that rely solely on raw images. High reliability: Through the confusion matrix, the system demonstrates superior ability to reduce false positives, which

is crucial for avoiding unnecessary maintenance costs in industrial facilities. As well as real-time performance to architecture optimization, the system achieves a response time of 42 milliseconds, allowing the robot to operate at 24 frames per second, ensuring continuous and accurate inspection without downtime. Future work includes subjecting the robot to field testing trials in actual industrial pipelines, expanding the size and variety of leakage samples under real-world flow conditions, and testing the direct experimental deployment of Edge AI on more powerful embedded processors such as NVIDIA Jetson.

REFERENCES

[1] Luo, X.H., Zhao, Y., Li, M.X., et al. (2025). Underground pipeline inspection and monitoring in mountainous areas: A state-of-the-art review and future perspectives. Tunnelling and Underground Space Technology, 164: 106783. https://doi.org/10.1016/j.tust.2025.106783

[2] Ma, Q.M., Liang, W.G., Zhou, P.Y. (2025). A review on pipeline in-line inspection technologies. Sensors, 25(15): 4873. https://doi.org/10.3390/S25154873

[3] Al-Sabaeei, A.M., Alhussian, H., Abdulkadir, S.J., Jagadeesh, A. (2023). Prediction of oil and gas pipeline failures through machine learning approaches: A systematic review. Energy Reports, 10: 1313-1338. https://doi.org/10.1016/j.egyr.2023.08.009

[4] Jona, A., Alkamachi, A. (2024). Design, modeling and PID control of a cable-driven wall climbing robot using genetic algorithms. Journal Européen des Systèmes Automatisés, 57(6): 1677-1685. https://doi.org/10.18280/JESA.570615

[5] Gros, J., Zatyagov, D., Papa, M., Colloseus, C., Ludwig, S., Aschenbrenner, D. (2023). Unlocking the benefits of mobile manipulators for small and medium-sized enterprises: A comprehensive study. Procedia CIRP, 120: 1339-1344. https://doi.org/10.1016/j.procir.2023.09.173

[6] Jawad, R., Jawad, R. (2024). Design and implementation of mobile robot for fire fighting using photovoltaic panel with artificial intelligent. Iranian Journal of Electrical and Electronic Engineering, 20(3): 117-126. https://doi.org/10.22068/IJEEE.20.3.3336

[7] Jawad, R., Jawad, R., Sabah Mohammed Ali, N., Sabah Mohammed Ali, E. (2025). An adaptive neuro-fuzzy inference system applied for the design of a firefighting robot using a photovoltaic panel. Journal of Applied Research and Technology, 23(5): 451-462. https://doi.org/10.22201/icat.24486736e.2025.23.5.2849

[8] Alfayizi, M.A. (2026). Traction-adaptive super-twisting sliding mode control for mecanum robotaxi tracking under wheel-speed constraints: Modeling, estimation, and benchmarking. Journal Européen des Systèmes Automatisés, 59(4): 925-941. https://doi.org/10.18280/JESA.590406

[9] Wang, Z.F., He, X.Q., Shen, H.L., Fan, S.J., Zeng, Y.L. (2022). Multi-source information fusion to identify water supply pipe leakage based on SVM and VMD. Information Processing & Management, 59(2): 102819. https://doi.org/10.1016/j.ipm.2021.102819

[10] Li, K.Y., Chen, W., Zou, Y.Y., Wang, Z.G., Zhou, X.Z., Shi, J.H. (2025). Optimized PSOMV-VMD combined with ConvFormer model: A novel gas pipeline leakage detection method based on low sensitivity acoustic signals. Measurement, 247: 116804. https://doi.org/10.1016/j.measurement.2025.116804

[11] Dai, Z.X., Li, S.Y., Liu, L., Zhu, Y.Q. (2024). Divisional intuitionistic fuzzy least squares twin SVM for pipeline leakage detection. Process Safety and Environmental Protection, 192: 104-114. https://doi.org/10.1016/j.psep.2024.10.045

[12] Sun, C.Y., Yan, Y., Zhang, W.B., Shao, D. (2024). Measurement of CO_2 leakage from pipelines under CCS conditions through acoustic emission detection and data driven modeling. Measurement, 237: 115164. https://doi.org/10.1016/j.measurement.2024.115164

[13] Xie, Y.W., Gao, M.Z., Luo, F., et al. (2025). Django-based framework database for leakage detection using machine learning for water distribution networks. Engineering Applications of Artificial Intelligence, 149: 110525. https://doi.org/10.1016/j.engappai.2025.110525

[14] Askari, M., Aliofkhazraei, M., Afroukhteh, S. (2019). A comprehensive review on internal corrosion and cracking of oil and gas pipelines. Journal of Natural Gas Science and Engineering, 71: 102971. https://doi.org/10.1016/j.jngse.2019.102971

[15] Abbasi, M., Shahraki, A., Taherkordi, A. (2021). Deep learning for network traffic monitoring and analysis (NTMA): A survey. Computer Communications, 170: 19-41. https://doi.org/10.1016/j.comcom.2021.01.021

[16] Levy, M., Naiser, F. (2019). Machine learning at the edge. In Software Engineering for Embedded Systems: Methods, Practical Techniques, and Applications, 2nd ed. Newnes, pp. 549-601. https://doi.org/10.1016/B978-0-12-809448-8.00015-1

[17] El Amoury, S., Smili, Y., Fakhri, Y. (2025). Design of an optimal convolutional neural network architecture for MRI brain tumor classification by exploiting particle swarm optimization. Journal of Imaging, 11(2): 31. https://doi.org/10.3390/jimaging11020031

[18] Jin, S.H., Son, D.M., Lee, S.H., Go, Y.H., Lee, S.H. (2025). Enhancing local contrast in low-light images: A multiscale model with adaptive redistribution of histogram excess. Mathematics, 13(20): 3282. https://doi.org/10.3390/math13203282

[19] Zhang, Q.C., Yang, L.T., Chen, Z.K., Li, P. (2018). A survey on deep learning for big data. Information Fusion, 42: 146-157. https://doi.org/10.1016/j.inffus.2017.10.006

[20] Alvarenga, A.V., Teixeira, C.A., Ruano, M.G., Pereira, W.C.A. (2010). Influence of temperature variations on the entropy and correlation of the grey-level co-occurrence matrix from B-mode images. Ultrasonics, 50(2): 290-293. https://doi.org/10.1016/j.ultras.2009.09.002

[21] Honeycutt, C.E., Plotnick, R. (2008). Image analysis techniques and gray-level co-occurrence matrices (GLCM) for calculating bioturbation indices and characterizing biogenic sedimentary structures. Computers & Geosciences, 34(11): 1461-1472. https://doi.org/10.1016/j.cageo.2008.01.006

[22] Gómez, W., Pereira, W.C.A., Infantosi, A.F.C. (2012). Analysis of co-occurrence texture statistics as a function of gray-level quantization for classifying breast ultrasound. IEEE Transactions on Medical Imaging, 31(10): 1889-1899.

https://doi.org/10.1109/TMI.2012.2206398
[23] Liu, X., Aldrich, C. (2022). Deep learning approaches to image texture analysis in material processing. Metals, 12(2): 355. https://doi.org/10.3390/met12020355
[24] Silik, A., Noori, M., Altabey, W.A., Ghiasi, R., Wu, Z.S. (2021). Comparative analysis of wavelet transform for time-frequency analysis and transient localization in structural health monitoring. Structural Durability & Health Monitoring, 15(1): 1-22. https://doi.org/10.32604/sdhm.2021.012751

NOMENCLATURE

a	GLCM Matrix Element
ANN	Artificial Neural Network
CNN	Convolutional Neural Network
CAD	Computer Aided Design
CLAHE	Contrast Limited Adaptive Histogram Equalization
DWT	Discrete Wavelet Transform
FDM	Fused Deposition Modeling
FN	False Negative
FNR	False Negative Rate
FP	False Positive
GLCM	Gray-Level Co-occurrence Matrix
LS-SVM	Least Squares Support Vector Machines
m	Mean
MSE	Mean Squared Error
N_2	Nitrogen Gas
PLA	Polylactic Acid
RF	Random Forest
s	Standard Deviation
SVM	Support Vector Machine
TN	True Negative
TP	True Positive
UART	Universal Asynchronous Receiver-Transmitter
VMD	Variational Mode Decomposition

Subscripts

i	row index
j	column index